

# Electric-Mechanical-Acoustic Coupling Characteristics for Pulse Tube Cryocoolers

L. Y. Wang, Z. H. Gan, Y. X. Guo, B. Wang, S. H. Wang

Institute of Refrigeration and Cryogenics, Zhejiang University  
Hangzhou 310027, P.R. China

Key Laboratory of Refrigeration and Cryogenic Technology of Zhejiang Province  
Hangzhou 310027, P.R. China

## ABSTRACT

A pulse tube cooler driven by a linear compressor can be equivalent to a network consisting of electric, mechanical and acoustic parts, among which the coupling is a critical issue for improving cooling performance. However, it is still a research area that remains poorly understood. In this work, we develop a coupled phasor diagram containing electric, mechanical and acoustic parts using a vector analysis method. The phasor analysis reveals the coupling characteristics inside a pulse tube cryocooler, especially the electric-to-acoustic conversion efficiency, the power factor, and so on. This is expected to help with the design and performance improvement of a pulse tube cryocooler.

## INTRODUCTION

Since the Oxford-style linear compressor was introduced by Davey in 1981, it has become a key element that ensures the high reliability and high efficiency of many Stirling-type cryocoolers.<sup>1,2</sup> For analysis purposes, the compressor can be divided into three parts: the electric, the mechanical, and the acoustic impedance parts.<sup>3,4</sup> The operation of the linear compressor comprises complex transition processes among these three parts. Coordination and coupling among each part are important for the cryocooler to achieve its best performance. Previous studies have reported on the dynamic characteristics of linear compressors, and the acoustic impedance on the piston was modeled using an equivalent damping coefficient and a gas spring stiffness.<sup>5,6</sup> Wakeland used an equivalent circuit model to analyze the performance and optimized the acoustic resistance under the resonant condition.<sup>3</sup> Swift also derived the efficiency using acoustic impedance analyses, and optimized the piston area at resonance.<sup>7</sup> Radebaugh et al. discussed the acoustic impedance match based on a given commercial linear compressor.<sup>8</sup> Dai et al. analyzed the impedance matching principle between the linear compressor and the cold head from the perspective of energy balance and derived the criteria for both maximizing the efficiency and maximizing power output.<sup>9</sup> Although much has been learned, some topics remain poorly understood. How to choose the best working condition for a given linear compressor? Are there any possible coupling methods in case the linear compressor does not match the cooler? And, how about the coupling characteristics among the entire electric-mechanical-acoustic parts?

This paper tries to answer these questions. A specific impedance point, called the ‘sweet spot’ is proposed aiming to obtain the highest efficiency as well as the maximum power output at the same

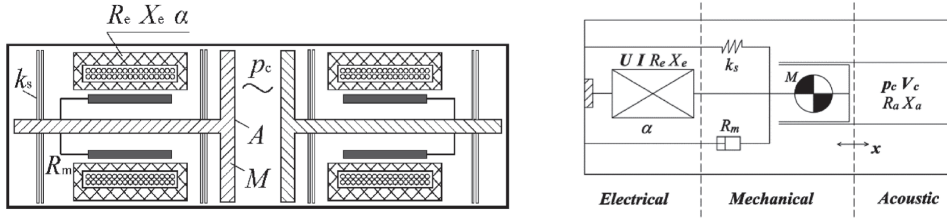


**Figure 1.** Schematic diagram and physical model of a linear compressor.

time. Some possible additional impedance matching methods are introduced based on an electrical impedance matching network. Finally, an electric-mechanical-acoustic coupling phasor diagram is introduced to analyze the coupling characteristics of the entire system.

### ‘SWEET SPOT’ FOR A LINEAR COMPRESSOR

The linear compressor shown in Fig. 1 is a kind of electrodynamic device that can be described by the following linear harmonic-approximation equations<sup>7</sup>:

$$\mathbf{U} = R_e \mathbf{I} + j\omega X_e \mathbf{I} + \alpha \mathbf{v} \quad (1)$$

$$M \mathbf{a} = \alpha \mathbf{I} - R_m \mathbf{v} - k_s \mathbf{x} - p_c A \quad (2)$$

where  $\mathbf{U}$  is the complex voltage across the electric terminals, with bold representing complex vectors,  $R_e$  is the electric resistance,  $\mathbf{I}$  is the complex electric current,  $X_e$  is the electric inductance,  $\alpha$  is the transduction coefficient which is the product of the magnetic field and the length of the wire in the field,  $\mathbf{x}$  is the piston displacement,  $\mathbf{v}$  is its velocity and  $\mathbf{a}$  is its acceleration,  $V_c$  is the volume flow rate at the piston face,  $p_c$  is the pressure amplitude inside the compression volume,  $R_a$  is the acoustic resistance and  $X_a$  is the acoustic reactance,  $A$  is the piston area,  $R_m$  is the mechanical resistance,  $j$  equals to  $\sqrt{-1}$ ,  $M$  is the moving mass,  $k_s$  is the mechanical spring stiffness. These two equations express Ohm's law and Newton's law, respectively.

We try to find a specific working condition for a given linear compressor to obtain its highest efficiency as well as maximum power output at the same time. To achieve the highest efficiency, both  $R_a$  and  $X_a$  should be fixed meeting the equations<sup>3</sup>:

$$A^2 X_a = \frac{k}{\omega} - m\omega \quad (3)$$

$$A^2 R_a = R_m \sqrt{\frac{\alpha^2}{R_e R_m} + 1} \quad (4)$$

where  $\omega = 2\pi f$  is angular frequency. To achieve the maximum power output, the following equation should be satisfied which means that the current and the displacement reaches their limits at the same time<sup>9</sup>:

$$\frac{\alpha I_{\max}}{\omega x_{\max}} = A^2 R_a + R_m \quad (5)$$

Combining Equations (3)–(5), we obtain

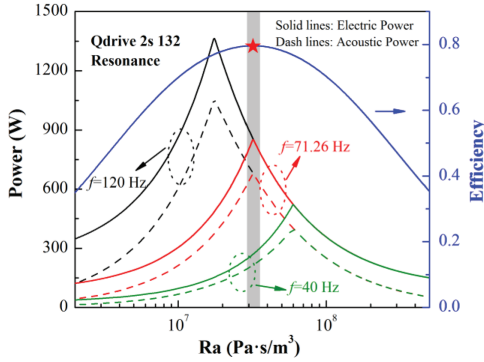
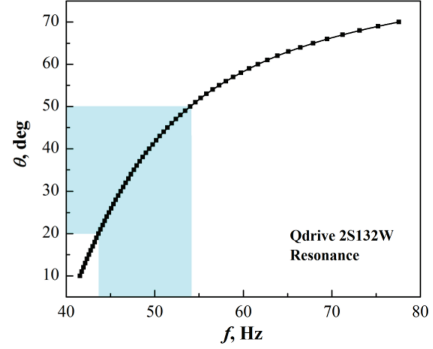
$$\frac{\omega}{\alpha} R_m \left( \sqrt{\frac{\alpha^2}{R_e R_m} + 1} + 1 \right) = \frac{I_{\max}}{x_{\max}} \quad (6)$$

In Equation (6), there is only one parameter that can be adjusted for a given linear compressor, that is the frequency  $\omega$ . Also, there is only one acoustic impedance point ( $R_a, X_a, f$ ) to meet this requirement. This specific impedance point is called the ‘sweet spot’ for a linear compressor.

Taking the existing commercial linear compressor Qdrive 2S132W<sup>10</sup> in our lab for instance, its parameters are listed in Table 1.

**Table 1.** Parameters of CFIC 2S132W linear compressor (single motor).

Parameters	$R_e$ ( $\Omega$ )	$k_s$ (N/m)	$R_m$ (N·s/m)	$\alpha$ (N/A)	$M$ (kg)	$d_p$ (m)	$I_{\max}$ (A)	$X_{\max}$ (mm)
Value	0.671	44800	10.7	23.5	0.721	0.0394	12.02	6.0

**Figure 2.** Efficiency and power for different frequencies under resonance of Qdrive 2S132W**Figure 3.** Phase angle vs. frequency under resonance of Qdrive 2S132W

Substituting these parameters from Table 1 into Equation (6), we get the specific frequency:

$$f = \frac{1}{2\pi} \frac{\alpha I_{\max}}{x_{\max} R_m \left( \sqrt{\frac{\alpha^2}{R_e R_m} + 1} + 1 \right)} = 71.26 \text{ Hz}$$

Calculations for three different frequencies (40 Hz, 71.26 Hz and 120 Hz) under resonance are carried out as shown in Fig. 2. The efficiency curves are overlapped, which means the efficiency has nothing to do with frequency as long as resonance is achieved. As for the power output, for all three frequencies, when  $R_a$  is small (e.g. less than about  $3.0 \times 10^7$  Pa·s/m³ for 71.26 Hz), the displacement reaches its upper limit before the current does; that is, the maximum displacement limits the power input and the power output. When  $R_a$  is large (e.g. larger than about  $3.0 \times 10^7$  Pa·s/m³ for 71.26 Hz), the current reaches its upper limit before the displacement does. In this case, the maximum current limits the power input and the power output. As a result, there is a specific  $R_a$  to reach the maximum power output for three frequencies ( $R_a$  meeting Equation (5)), and the higher the frequency is, the higher the maximum power output will be among these frequencies. The 71.26 Hz frequency is the one where the highest efficiency accompanies the maximum power output; this is the frequency the linear compressor should work at so as to fulfill its capability.

However, we note that the rated working frequency of this compressor is 60 Hz<sup>10</sup>, which was also used in our previous work.<sup>11</sup> We turn to the cryocooler side to see how this frequency affects the phase angle  $\theta$  between mass flow and pressure wave at the compressor outlet. For the acoustic impedance we have:

$$X_a = -R_a \tan \theta \quad (7)$$

Combining the resonant Equation (3), we obtain the relation between  $f$  and  $\theta$ :

$$f = \frac{1}{2\pi} \frac{1}{2M} \left[ A^2 R_a \tan \theta + \sqrt{A^4 R_a^2 \tan^2 \theta + 4Mk_s} \right] \quad (8)$$

To achieve the highest efficiency, Equation (4) should be satisfied. By substituting parameters from Table 1, we obtain the relation between  $f$  and  $\theta$ , as shown in Fig. 3. It is found that  $\theta$  increases as  $f$  increases. Generally,  $\theta$  should be between 20–50 degrees (mass flow leading the pressure wave) for a cryocooler, which needs the  $f$  to be between about 43–54 Hz in this case shown from Fig. 3. But this frequency region is lower than the ‘sweet’ frequency 71.26 Hz, which means that

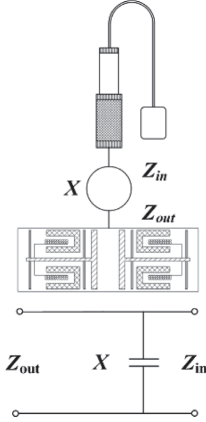


**Figure 4.** Extra volume matching and its equivalent circuit.

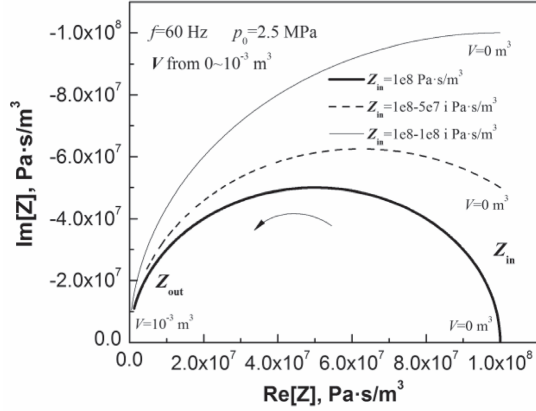


**Figure 5.** Effects of extra volume on  $Z_{out}$ .

power output is limited as shown from Fig. 2. On the other hand, if driving the linear compressor at 71.26 Hz,  $\theta$  will be much larger for the cryocooler according to Fig. 3. This is one of the cases that mismatch between the linear compressor and the cryocooler occurs; here extra matching methods are needed.

### POSSIBLE IMPEDANCE MATCHING METHODS

Additional matching methods are needed to ensure high efficiency of both the linear compressor and the cryocooler, and no extra dissipation is expected to be introduced. The most simple way is to add a buffer volume between them (in series or in parallel). Figure 4 shows the structure and its equivalent circuit. Here  $Z_{in}$  is the acoustic impedance of the cooler,  $X$  is the reactance of the volume, and  $Z_{out}$  is the acoustic impedance at the compressor outlet. We have the equation:

$$Z_{out} = \frac{1}{1/Z_{in} + 1/X} \quad (9)$$

We calculate the effects of volume ( $0 \sim 10^{-3} \text{ m}^3$ ) on  $Z_{out}$  for different  $Z_{in}$ , as shown in Fig. 5. It is seen that the extra volume can adjust the acoustic impedance in a quite wide range, but for each  $Z_{in}$ ,  $Z_{out}$  will vary along a specific curve as the volume increases. This matching method can not realize the impedance match between an original  $Z_{in}$  and an arbitrary  $Z_{out}$ .

In the electronics field, an impedance matching network is widely used.<sup>12</sup> Here we introduce the simple  $L$  type double component impedance matching network. The four possible matching structures and their equivalent circuits are shown in Fig. 6, in which the buffer volume is analogous to electric capacitance and the inertance tube is analogous to electric inductance.

These matching networks have a much wider impedance adjusting range (other than a specific curve). Taking the first network in Fig. 6 as an example, it is described by the following equation:

$$Z_{out} = \frac{1}{1/Z_{in} + i\omega C} + i\omega L \quad (10)$$

where  $C$  is the acoustic capacitance of the volume, and  $L$  is the acoustic inertance of the inertance tube. Writing  $Z_{in}$  and  $Z_{out}$  in the forms:

$$\begin{aligned} Z_{in} &= R_{in} + iX_{in} \\ Z_{out} &= R_{out} + iX_{out} \end{aligned} \quad (11)$$

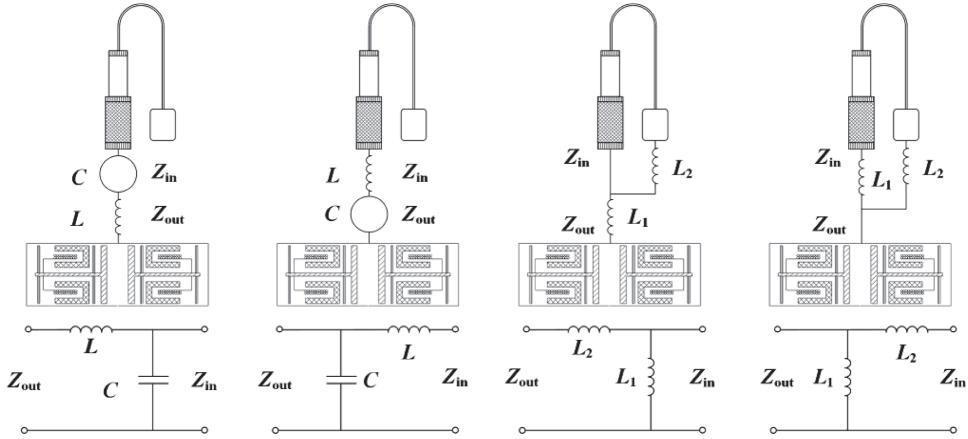


**Figure 6.** Four  $L$  type impedance matching networks and their equivalent circuits

By substituting Equation (11) into Equation (10), we can derive the required  $C$  and  $L$ :

$$C = \frac{1}{\omega} \frac{X_{in} \pm \sqrt{\frac{R_{in}}{R_{out}} (R_{in}^2 + X_{in}^2) - R_{in}^2}}{R_{in}^2 + X_{in}^2} \quad (12)$$

$$L = \frac{1}{\omega} \left[ \frac{1}{\omega C} - \frac{R_{out} (1 - \omega C X_{in})}{\omega C X_{in}} + X_{out} \right]$$

That is, for any given  $Z_{in}$  and  $Z_{out}$ ,  $Z_{out}$  could be achieved at the compressor outlet by using the  $L$  type impedance matching network with  $C$  and  $L$  calculated from Equation (12). There are still some forbidden zones that can not be reached; these are not discussed in this paper.

## ELECTRIC-MECHANICAL-ACOUSTIC COUPLING

In a Stirling-type cryocoolers driven by a linear compressor, most parameters inside are sinusoidal. Thus, a phasor analysis provides a convenient way to describe the phase relationship between mass flow and pressure wave inside the cooler<sup>13</sup>, the forces acting on the piston<sup>14</sup>, as well as the voltage balance within the electric elements.<sup>15</sup>

For the voltage balance, Equation (1), the first term on the right side represents the voltage drop in the electric resistance that is in phase with current. The second term on the right side represents the voltage change due to electric inductance, which is  $90^\circ$  out of phase with current. The third term on the right side represents the induced voltage due to the piston movement, which is in phase with piston velocity. Figure 7(a) shows the phasors of each term in the complex frequency domain, in which  $I$  is chosen to be the  $x$ -axis. The sum of the above three vectors is the total voltage  $U$ . It should be noted that the phase angle between  $U$  and  $I$ ,  $\psi$ , has a cosine value known as the power factor.

In the force balance, Equation (2), the inertial force  $Ma$  is in phase with piston acceleration. For each term on the right side, the motor force  $\alpha I$  is in phase with current, the damping force  $R_m v$  is in phase with piston velocity, the mechanical spring force  $k_s x$  is in phase with piston displacement, and the gas force  $p_c A$  is in phase with pressure wave. Figure 7(b) shows the phasors of each term in the complex frequency domain, in which  $x$  is chosen to be the  $x$ -axis. Here the phase angle between  $v$  and  $I$ ,  $\beta$ , is a critical angle for a linear compressor. When  $\beta = 0$ , the motor force is minimized for the same power output, which means the highest efficiency is obtained; this condition is known as resonance. What's more, the phase angle between  $v$  and  $p_c$ ,  $\phi$ , depends on the particular cold head attached to the compressor. For the cold head side, according to the equation for conservation of

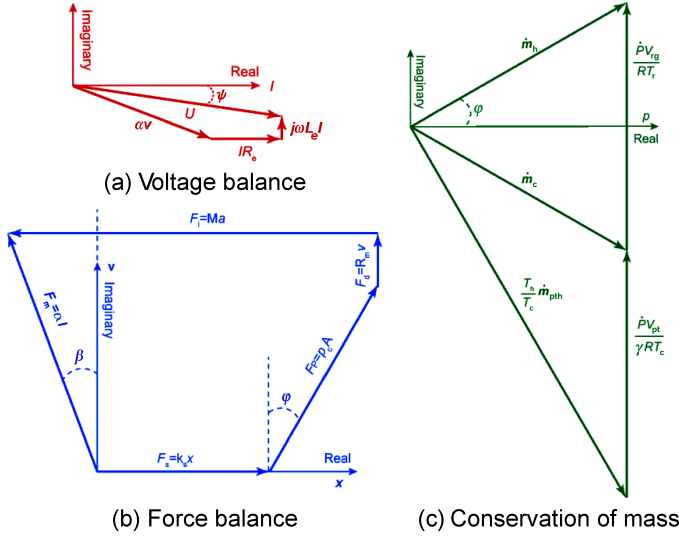


Figure 7. Phasor diagrams of electric, mechanical and acoustic parts.

mass, we have<sup>13</sup>:

$$\dot{m}_h = \dot{m}_c + \frac{\dot{P}V_{reg}}{RT_a} \quad \dot{m}_c = \frac{T_{ht}}{T_c} \dot{m}_{ht} + \frac{\dot{P}V_{pt}}{\gamma RT_c} \quad (13)$$

where  $\dot{m}$  is mass flow rate,  $\dot{P}$  is the rate of change of pressure wave,  $V$  is the gas volume of the element,  $R$  is the gas constant per unit mass,  $T_a$  is the average temperature in the component,  $\gamma$  is the ratio of the specific heats, subscripts  $h, c, ht, reg, pt$  means hot end of the regenerator, cold end, hot end of the pulse tube, regenerator, pulse tube, respectively. According to Equation (13), we obtain the phasor diagram of the mass flow and pressure wave in the cold head, shown as Fig. 7(c). Here, to achieve the best performance of a regenerator, generally the optimum phase relationship is that  $\dot{m}$  and  $p$  are in phase at approximately the midpoint of the regenerator.<sup>16</sup> Typically the flow at the cold end will lag the pressure by about 30°, whereas at the warm end the flow leads the pressure by about 30°. To meet such a phase relationship, the flow will always lag the pressure by about 60° at the warm end of the pulse tube, as shown in Fig. 7(c). Here the phase angle between  $\dot{m}$  and  $p$  at the hot end of the regenerator,  $\varphi$ , is same as that in Fig. 7(b).

All the analyses above are in the same complex frequency domain. It would be helpful to combine the three phasor diagrams together, to see how the different parts couple with each other. Fig. 8 shows the joint phasor diagram of the entire electric–mechanical–acoustic parts in a cryocooler which is a combination of the three diagrams from Fig. 7. In this figure, the electric and mechanical parts are coupled by  $v$  and  $I$ , while the mechanical and acoustic parts are coupled by  $v$  ( $\dot{m}$ ) and  $p_c$ . The relative magnitudes of different parts are only schematic.

Figure 8 is helpful in the design, analysis and optimization of a cryocooler, especially in the understanding of coupling among the three different parts. For example, on the one hand, in order to ensure good cooling performance of the cold head, the phase angle  $\varphi$  should be around 30°. This in turn requires a reasonable design of the linear compressor so as to maintain such a phase relationship between  $v$  and  $p_c$ . On the other hand, the linear compressor should work around the resonance to get its highest efficiency; this needs the phase angle  $\beta$  to be near 0°. The requests above can be satisfied by adjusting the parameters in the compressor, e.g.  $M, k_s, A$ .

In some applications, people are concerned about the power factor (that is the phase angle  $\psi$ ). It is noted from Figure 8 that  $\psi = 0$  and  $\beta = 0$  can not occur at the same time as long as  $L_c \neq 0$ , that is, power factor equals 1 doesn't mean resonance and vice versa.<sup>4</sup> Sometimes attention should also be paid to power factor to avoid too high a voltage. In this case, the compressor efficiency should be sacrificed a little ( $\beta \neq 0$ , and  $v$  leading  $I$ ).

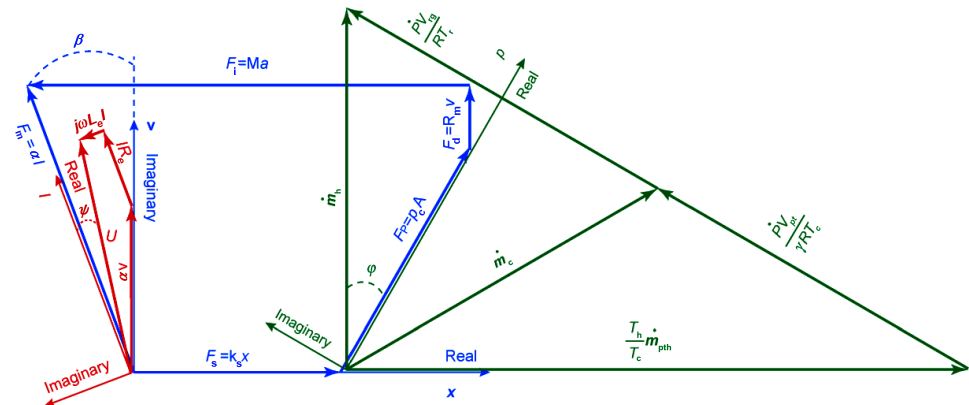


Figure 8. Joint electric-mechanical-acoustic coupling phasor diagram

All the discussions here are aimed at the phase angles in Fig. 8. Similar coupling analyses can also be done specific to magnitudes of each vector. Figure 8 reveals the intrinsic coupling mechanism between different parts, and provides references for reaching the best performance of a Stirling-type cryocooler.

CONCLUSIONS

Study on the coupling characteristics of a cryocooler is carried out. In order to fulfill the capability of a linear compressor, it should be operated around such a ‘sweep spot’ to obtain the highest efficiency and maximum power output at the same time. Several possible impedance matching methods in analogy with electrical matching networks are introduced if the compressor doesn’t match the cold head. A joint electric-mechanical-acoustic coupling phasor diagram is achieved. It reveals the intrinsic coupling mechanism between different parts and provides references for reaching the best performance of a Stirling-type cryocooler.

ACKNOWLEDGMENTS

This work is financially supported by the National Natural Science Foundation of China (No. 51376157) and the Specialized Research Fund for the Doctoral Program of Higher Education of China (No. 20130101110098). The authors would like to express their gratitude to Dr. Ray Radebaugh for his helpful discussion at Zhejiang University.

REFERENCES

1. Davey, G., “The Oxford University Miniature Cryogenic Refrigerator,” *International Conference on Advanced infrared detectors and systems*, (1981), pp. 39.
2. Davey, G., “Review of the Oxford Cryocooler,” *Adv. in Cryogenic Engineering*, Vol. 35B, Plenum Publishing Corp., New York (1990), pp. 1423-1430.
3. Wakeland, R.S., “Use of Electrodynamic Drivers in Thermoacoustic Refrigerators,” *Journal of the Acoustical Society of America*, vol. 107, no. 2 (2000), pp. 827-832.
4. Gan, Z.H., Wang L.Y., Zhao S.Y., Song Y.J., Wang W.W., and Wu Y.N., “Acoustic Impedance Characteristics of Linear Compressors,” *Journal of Zhejiang University-Science A*, vol. 14, no. 7 (2013), pp. 494-503.
5. Koh, D.Y., Hong Y.J., Park S.J., Kim H.B., and Lee K.S., “A Study on the Linear Compressor Characteristics of the Stirling Cryocooler,” *Cryogenics*, vol. 42, no. 6-7 (2002), pp. 427-432.
6. Chen, N., Tang Y.J., Wu Y.N., Chen X., and Xu L., “Study on Static and Dynamic Characteristics of Moving Magnet Linearcompressors,” *Cryogenics*, vol. 47, no. (2007), pp. 457-467.

7. Swift, G., *Thermoacoustics: A Unifying Perspective for Some Engines and Refrigerators*. 2002, Los Alamos National Laboratory: Acoustical Society of America Publications.
8. Radebaugh, R., Garaway I., and Veprik A.M., "Development of Miniature, High Frequency Pulse Tube Cryocoolers," *Proc. SPIE 7660, Infrared Technology and Applications XXXVI*, 76602J (4 May 2010); doi: 10.1117/12.852766.
9. Dai, W., Luo E.C., Wang X.T., and Wu Z.H., "Impedance Match for Stirling Type Cryocoolers," *Cryogenics*, vol. 51, no, 4 (2011), pp. 168-172.
10. <http://www.Chartindustries.Com/Industry/Industry-Products/Gas-Systems/Qdrive/Qdrive-Products/Pressure-Wave-Generators/Pressure-Wave-Generators-2s132w>.
11. Wang, L.Y., Wu M., Sun X., and Gan Z.H., "A Cascade Pulse Tube Cooler Capable of Energy Recovery," *Applied Energy*, vol. 164, no, (2016), pp. 572-578.
12. Matthaei, G., Jones E.M.T., and Young L., *Microwave Filters, Impedance-Matching Networks, and Coupling Structures*. Artech Microwave Library. 1980: Artech House.
13. Radebaugh, R., "Thermodynamics of Regenerative Refrigerators," *Generation of Low Temperature and It's Applications*, (2003), pp. 1-20.
14. Marquardt, E. and Radebaugh R., "Design Equations and Scaling Laws for Linear Compressors with Flexure Springs," *7th International Cryocooler Conference Proceedings*, Air Force Phillips Laboratory Report PL-CP--93-1001, Kirtland Air Force Base, NM, April 1993, pp. 783-804.
15. Radebaugh, R., Lewis M., and Bradley P., "Verification of the Back-Emf Method for Piston Velocity Measurements," *Cryocoolers 17*, ICC Press, Boulder, CO (2012), pp. 357-365.
16. Radebaugh, R., Lewis M., Luo E., Pfothhauer J.M., Nellis G.F., and Schunk L.A., "Inertance Tube Optimization for Pulse Tube Refrigerators," *Advances in Cryogenic Engineering, Vols 51A and B*, Amer. Institute of Physics, Melville, NY (2006), pp. 59-67.